J Nanopart Res (2020) 22: 307
https://doi.org/10.1007/s11051-020-05037-9

RESEARCH PAPER

Synthesis and physicochemical characterization of rhamnolipid-stabilized carvacrol-loaded zein nanoparticles for antimicrobial application supported by molecular docking

Ngangom Bidyarani · Amit Kumar Srivastav · Sanjeev K. Gupta · Umesh Kumar

Received: 9 July 2020 / Accepted: 2 October 2020 / Published online: 8 October 2020

Abstract Carvacrol is a phenolic monoterpenoid obtained from the genera of *Origanum*, *Thymus*, *Satureja*, and *Lippia*. It is a hydrophobic phytoconstituent that readily tends to decay while processing leading to restricting its potential application. In the current study, zein/rhamnolipid (ZRL of 306 nm) complex nanoparticles were loaded with carvacrol successfully (CRZRL of 271 nm) to explore its antimicrobial activity and obtained the MIC value of 135 μg/ml and 270 μg/ml against *P. syringae* (bacterial canker) and *F. oxysporum* (Fusarium wilt) respectively. These complex nanoparticles were further characterized by DLS, FE-SEM, DSC, FT-IR, H^1NMR, docking, and HPLC studies. The strong interaction of carvacrol with zein and rhamnolipid complex nanoparticles which showed characteristic peaks in FTIR as well as H^1NMR were also supported by our docking studies. This strong interaction resulted in higher EE (95%) as well as LE (42%), confirmed by HPLC studies. Docking studies further revealed the presence of stronger Π-Π interaction within binding and active sites of zein through which rhamnolipid and carvacrol interact. The developed nano-formulation could be exploited for controlling different plant diseases and other foodborne pathogens.

Keywords Carvacrol · Rhamnolipid · Antimicrobial activity · Zein · Docking

Electronic supplementary material The online version of this article (https://doi.org/10.1007/s11051-020-05037-9) contains supplementary material, which is available to authorized users.

N. Bidyarani · A. K. Srivastav · U. Kumar (✉)
School of Nano Sciences, Central University of Gujarat, Gandhinagar, Gujarat 382030, India
e-mail: umesh.kumar@cug.ac.in

S. K. Gupta
Computational Materials and Nanoscience Group, Department of Physics, St. Xavier's College, Ahmedabad 380009, India

Introduction

Management and control of plant diseases and foodborne pathogens associated with vegetables and other important crops have become very crucial in the current scenario due to the enormous number of pests, insects, and microbes affecting the productivity or yield. Chemicals such as plant growth regulators, fertilizers, and pesticides are required in large amounts to increase food production for continuously feeding the rising human population (Hirano and Upper 2000; van der Wolf and De Boer 2015). Crops are widely destroyed by the phytopathogenic microorganisms leading to the cause of various plant diseases. Some plant diseases like necrosis, canker, and wilt are caused by bacteria and fungi and they are reproduced very easily in plants (Casas-Flores et al. 2019). Phytopathogenic microorganisms like *Pseudomonas syringae* and *Fusarium oxysporum* infects various plants extensively, causing blight, speck, root rot, and wilt in different crops including tomato, banana, rice, sweet potatoes, legumes, etc.

Various chemicals including bactericides, fungicides, pesticides, etc. and also methods like UV light treatment, peroxide oxidation, chlorination, etc. have been used to control microbial infections on vegetables, crops, cereals, and grains (Hirano and Upper 2000; Fones and Preston 2013; van der Wolf and De Boer 2015) but its application in the proper amount is very essential for safety purpose to both human and environment. Several steps and measurements have been implemented to control the plant pathogenic microorganisms and the associated diseases. Among the various steps, nanotechnology-assisted synthesis of nanoformulation using phytoconstituents could be a boon to the serious concerns raised by microbial infections causing different plant and foodborne diseases.

Carvacrol is a phenolic monoterpene that is a primary phytoconstituent of several essential oils extracted from oregano having antimicrobial (Del Nobile et al. 2008; Guarda et al. 2011), antioxidant (Camo et al. 2011), and anti-inflammatory (Riella et al. 2012) properties. Its application as food additives and an alternative to synthetic additives are well established (Mastromatteo et al. 2010; Ramos et al. 2012) but the major limitation is retaining its bioactivity for a longer period. Many previous studies have reported the antimicrobial activity of carvacrol and carvacrol loaded nanoparticles against various gram-positive (*B. cereus*, *L. monocytogenes*, *S. aureus*, etc.) (da Rosa et al. 2015) and gram-negative (*E. coli*, *Salmonella*, *S. enterica*, etc.) (Keawchaoon and Yoksan 2011) bacteria including fungi (*B. cinerea*, *Aspergillus* spp., *Cladosporium* spp., etc.) (Martínez-Romero et al. 2007; Abbaszadeh et al. 2014) but its activity against phytopathogenic microbes like *P. syringae* and *F. oxysporum* is yet to be reported. The method of encapsulation in polymer or protein matrices is an alternative to maintain its stability, bioactivity, and retain its intrinsic properties (da Rosa et al. 2015). Zein is a corn prolamine, rich in amino acids such as proline, leucine, glutamine, and alanine. Hydrophobicity makes zein capable of self-assembling in the presence of polar solvents like water, which has already been used to encapsulate rotenone, essential oils, including oregano, thyme, thymol, curcumin, and carvacrol (Wu et al. 2012; Paliwal and Palakurthi 2014; Devi et al. 2019). Zein acts as a promising agent to develop various nanoformulations since it is biocompatible, biodegradable, less toxic, and cost-effective (Li et al. 2017; de Oliveira et al., 2018). Zein nanoparticles have been known for their low encapsulation and loading efficiencies. Thus, the fabrication of zein nanoparticles by coating or complexing with polysaccharides, proteins, and small molecular weight emulsifiers (Dai et al. 2018) proved to be a very effective technique for enhancing these attributes. In our previous study, zein has been complexed with sodium caseinate using an antisolvent precipitation method (Devi et al. 2019) but in our present study, we used an alternative promising way to encapsulate carvacrol using rhamnolipid, a biosurfactant to form a stable complex with zein for controlling the infection caused by phytopathogenic microorganisms.

Rhamnolipid is a type of glycolipid produced by bacteria, *Pseudomonas aeruginosa* (Dwivedi et al. 2015). It generally consists of one or two polar rhamnose units and one nonpolar fatty acid chain containing a β-hydroxylalkanoate, leading to an anionic character (Bai and McClements 2016). Rhamnolipids show a good emulsifying behavior because of their amphiphilic nature and used in food-grade emulsion extensively (Bai and McClements 2016). Researchers have reported that rhamnolipids could stabilize o/w nanoemulsions containing small droplets of curcumin for nutraceutical application, against a range of temperatures, salt concentrations, and different pH (Dai et al. 2018) but extensive studies are required for exploring rhamnolipids as a stabilizer to improve the encapsulation and loading efficiencies of the protein nanoparticles. We hypothesized to develop a completely green approach towards the synthesis of nano-formulation where each component is either derived from plants (zein) or microorganisms (rhamnolipid), making it a completely biodegradable system for controlling plant pathogens or other foodborne pathogens.

To achieve this, we fabricated zein nanoparticles using rhamnolipid to encapsulate carvacrol, enhancing its encapsulation as well as loading efficiencies and explored its efficacy against plant pathogens, e.g., *P. syringae* and *F. oxysporum*. These microbes cause mainly bacterial canker, necrosis, and Fusarium wilt to many important crops including vegetables and fruits. Till date, there are no reported studies where each single component of the nanocarrier, i.e., matrix, active ingredient, and stabilizing agent is either derived from plants or of biological origin, have been utilized in the form of biodegradable nano-formulation for controlling plant pathogens. Exploration of such biodegradable nano-formulation is the need of hour to control various plant diseases causing microorganisms in a sustainable

manner. Thus, we can say that the prepared nanoformulation could help in managing certain pant diseases of important crops and also able to assist in food production (by preventing the crop yield loss from microbial attack) for the continuously rising human population. The characteristics of the fabricated complex nanoparticles were explored in terms of size, stability by DLS, structural and functional characters by H^1NMR, FTIR, morphology by FE-SEM, and encapsulation and loading efficiencies by HPLC. Furthermore, to improve our understanding about the molecular interaction between zein/rhamnolipid matrix and an active ingredient like carvacrol we used molecular docking studies to find the actual amino acid residue within the matrix responsible for binding with carvacrol which is very crucial for regulating the loading and encapsulation efficiency by controlling pH, ionic strength, electrostatic interaction, etc., of protein (Srivastav et al. 2020). The present study gives a new insight to control plant infection and disease caused by *P. syringae* and *F. oxysporum* in an environment-friendly manner.

Materials and methods

Materials

Zein (Z 3625; CAS Number: 9010-66-6), carvacrol (282,197; 98%; CAS number 499-75-2), and rhamnolipid (R90, 90%) were purchased from Sigma Aldrich. Ethanol was purchased from the Bioscience laboratory. Nutrient agar (NA), potato dextrose agar (PDA), nutrient broth (NB), and potato dextrose broth (PDB) were obtained from Himedia laboratories. *Pseudomonas syringae* was obtained from Junagadh Agricultural University, and *Fusarium oxysporum* was purchased from the division of plant pathology, IARI, New Delhi. All the solvents and chemicals used were of analytical grade. A syringe filter was obtained from Axiva.

Preparation of zein/rhamnolipid complex nanoparticles (ZRL) and carvacrol-loaded zein nanoparticles (CRZRL)

ZRL and CRZRL were prepared by antisolvent precipitation with slight modifications (Dai et al. 2018). Zein was dissolved in an aqueous ethanol solution of 85% (v/v) and stirred overnight at room temperature (25 °C). The prepared zein solution was filtered through a 0.45-μm syringe filter. ZRL was prepared and optimized considering different ratios (w/w) of zein and rhamnolipids. The different zein and rhamnolipid mass ratio were 1:0.5, 1:1, and 1:2 denoted as ZRL. The filtered zein solution and carvacrol solution (carvacrol dissolved in absolute ethanol) were mixed and dissolved in aqueous ethanol (85%, v/v) to reach a concentration of 0.9 mg/mL of carvacrol, with magnetic stirring at 600 rpm at room temperature for 1 h. Then rhamnolipid was added into the zein and carvacrol-mixed solution and continued the stirring (600 rpm) for further 2 h to obtain a homogenous colloidal suspension (CRZRL). The prepared colloidal suspension was freeze-dried for 24 h and used for further physicochemical and morphological characterizations using different techniques.

Hydrodynamic size, polydispersity index, and zeta potential measurement

The hydrodynamic size, polydispersity index (PDI), and zeta potential of the freshly prepared samples were measured using the Metrohm DLS instrument. The samples were prepared at 25 °C, and signals with a backscattering angle of 173° were captured for data generation. Two hundred microliters of the prepared samples were diluted 20 times with Milli Q water and then samples were sonicated for 15 min. A cumulative mean diameter was obtained as particle size (hydrodynamic size, nm). The polydispersity index (PDI) and zeta potential were also thus obtained. All measurements of the samples were examined in triplicate.

Encapsulation and loading efficiency (EE% and LE%) by high-performance liquid chromatography (HPLC)

The EE and LE of CR in the nanoparticles were estimated as reported (Zhang et al. 2014). The freshly prepared CRZRL was centrifuged at 6000 rpm for 20 min at 4 °C to evaluate the amount of carvacrol. The encapsulated amount of carvacrol was measured using Jasco PU-2080 Plus. The method of analysis was optimized by using HPLC grade water, methanol, and acetic acid at a volume ratio of 30:70:3 as a mobile phase in an isocratic mode at a flow rate of 1 mL/min. The amount of sample injected was 20 μL and the absorbance was detected at 274 nm at 17.4 min (retention time). The carvacrol concentration was determined based on the sample peak area and the measurement was conducted in triplicate.

The encapsulation efficiency (EE) and loading efficiency (LE) were calculated using Eqs. 1 and 2, respectively.

$$EE\% = \frac{\text{Encapsulated carvacrol } (\mu g)}{\text{Total initial carvacrol } (\mu g)} \times 100 \quad (1)$$

$$LE\% = \frac{\text{Encapsulated carvacrol } (\mu g)}{\text{Total weight of zein and rhamnolipid } (\mu g)} \times 100 \quad (2)$$

Field emission scanning electron microscopy (FE-SEM)

The surface morphology of the prepared CRZRL and ZRL was characterized using FESEM (Zeiss ultra 55 FESEM). Ten microliters of sonicated colloidal solution (CRZRL and ZRL) dropped cast on a silicon wafer, attached to SEM stubs using carbon tape. The samples were sputter-coated with gold-palladium mixture under vacuum for 5 min before measurement and were evaluated by FESEM, operated at an accelerating voltage of 10 kV.

Thermal stability by differential scanning calorimeter (DSC)

The thermal degradation and shifting, if any, in the endothermic peaks (thermograms) of CR, ZRL, CRZRL, and RL were studied by DSC (Perkin Elmer, DSC 6000). Previously lyophilized samples were weighed approximately 5 mg in an aluminum pan. The samples were heated in the aluminum pan at the rate of 10 °C min^{-1}, with 20 mL min^{-1}nitrogen flow. The samples were analyzed at temperatures between 55 and 300 °C. An empty sealed aluminum pan was used as a baseline.

Fourier transform infrared spectroscopy (FTIR)

To confirm the functional groups in pure carvacrol (CR), rhamnolipid (RL), ZRL, and CRZRL, were performed through FTIR (Perkin Elmer Spectrum 65). The KBr pellet was run as a baseline and mixed with the sample in a ratio of 1:99. The analysis was recorded over 64 cumulative scans in the wavenumber between 4000 and 400 cm^{-1}, with a 4 cm^{-1} resolution limit.

Proton nuclear magnetic resonance spectroscopy (^{1}HNMR) analysis

The various types of hydrogen bonds present in pure carvacrol (CR), rhamnolipid (RL), ZRL, and CRZRL were studied using ^{1}HNMR spectroscopy, Bruker 500-MHz Ultra shield plus NMR instrument. Each sample of approximately 5 mg was dissolved in deuterated chloroform ($CDCl_3$). The ^{1}H NMR analysis was carried out at 298 K and frequency 500 MHz.

Molecular docking studies

In the current study, the interaction among the compounds, carvacrol, and rhamnolipid with the zein protein were performed in-silico to determine the binding affinity and active targeting or binding sites. All 2D and 3D structure of the compounds or drug was obtained from the PubChem database (https://pubchem.ncbi.nlm.nih.gov/). The zein protein structure was generated from the FASTA sequence of the PDB database for docking studies. Auto Dock Vina software was used to investigate the molecular interaction among carvacrol, rhamnolipid, and zein protein (Trott and Olson 2010). The Lamarckian genetic algorithm was used to analyze the probability of docking studies (Fuhrmann et al. 2010). Docking results were analyzed by Autodock 4.2, pymol version.

Antimicrobial activity

P. syringae and *F. oxysporum* are plant pathogenic gram-negative bacteria and fungi respectively procured from Junagadh Agricultural University, Gujarat, and Division of plant pathology, IARI, New Delhi. The microorganisms were cultured in their respective media with their optimum 1×10^6–10^7 CFU/mL (*P. syringae*) and 2000 spores count (*F. oxysporum*) as reported earlier (Broekaert et al. 1990; Zhang et al. 2014). The selected organisms have been studied in our previous work (Devi et al. 2019) but the effect of carvacrol against these selected plant pathogenic microorganisms (*P. syringae* and *F. oxysporum*) has not been reported yet as per our knowledge. So, we intended to study the efficacy of this developed nanoformulation against *P. syringae* and *F. oxysporum.* Antibacterial activity of

CRZRL was studied at different concentrations ranging from 45 to 225 μg/mL while for antifungal activity the concentration range was 90–450 μg/mL. The final volume was made up to 250 μL with nutrient broth (NB) and potato dextrose broth (PDB) in each well of the 96-well microplate for antibacterial and antifungal studies respectively. *P. syringae* and *F. oxysporum* suspensions without adding any samples (ZRL, CRZRL, and CR) were kept as the negative control (NC as included in Fig. 6a. b). The minimum inhibitory concentration (MIC) value of CRZRL was determined by the broth dilution method with some modifications (Weerakkody et al. 2010; Zhang et al. 2014). The readings for antibacterial activity against *P. syringae* and antifungal against *F. oxysporum* were measured at 600 nm from 0 to 24 h and 595 nm from 24 to 120 h respectively at different time intervals using a Biotek synergy hybrid microplate reader. The plate assay of the antibacterial and antifungal activity was given in Figs. ES1 and ES2 as Supporting Information and the details of the methodology already reported in our previous study (Devi et al. 2019). Each sample measurement was prepared and studied in triplicate for both antibacterial and antifungal assay.

Results and discussion

Hydrodynamic size, polydispersity index (PDI), and zeta potential measurement

Table 1 shows the cumulative mean of particle size, PDI, and zeta potential measured from DLS studies of ZRL at different (zein:rhamnolipid) mass ratio of 1:0.5, 1:1, and 1:2 and carvacrol-loaded CRZRL. Among the various recorded DLS data, ZRL with zein:rhamnolipid mass ratio of 1:1 was considered for further studies based on PDI and zeta potential as 1:1 ratio showed monodispersed particles indicating less aggregation and higher stability. Thus, ZRL with zein:rhamnolipid mass ratio of 1:1 was further used for encapsulating carvacrol.

CRZRL showed 276 ± 10 nm particle size with 0.24 ± 0.07 PDI and − 29.13 ± 1.60 mV zeta potential which is lesser in particle size and higher zeta potential as compared to ZRL. This may be due to the interaction of phytoconstituents in the dispersion acting as a better stabilizing agent and thus preventing the particles from aggregating to larger particle size (Rhein et al. 2006; da Rosa et al. 2015). This was quite evident visually by the fact that ZRL started showing precipitation whereas CRZRL was as it is even after 45 days of storage. The PDI value lesser than 0.3 indicates a narrow size distribution and well-dispersed homogeneity of the formulations (Wu et al. 2012). The negative polarity of the surface particle charge was due to the rhamnolipid as per the previous report (Dai et al. 2018) and this negative charge will keep on increasing with a higher amount of rhamnolipid. Zeta potential (mV) generally evaluates the stability of the colloidal dispersion. As rhamnolipid is an anionic biosurfactant so negative charge was observed. The higher zeta potential in CRZRL (− 29.13 ± 1.60 mV) as compared to ZRL (− 24.61 ± 1.71 mV) could be due to strong electrostatic repulsion of carvacrol with zein and rhamnolipids (da Rosa et al. 2015). The current study shows a biosurfactant, rhamnolipids with carvacrol provide better stability causing a steric hindrance in the external layer nanoparticles leading to higher zeta potential and lower particle size of the carvacrol-encapsulated nanoparticles.

Encapsulation and loading efficiency (EE% and LE%) calculation by HPLC

Encapsulation and loading efficiency are the main parameters to evaluate the affinity of the carvacrol (phytoconstituents) towards the zein and rhamnolipid complex nanoparticles which proved to be a better

Table 1 Particle size, PDI, and zeta potential of ZRL with different mass ratios (zein:rhamnolipid) and the encapsulation and loading efficiency (EE% and LE%) of carvacrol-loaded zein nanoparticles (CRZRL) as per DLS studies

Sample	Hydrodynamic size (nm)	PDI	Zeta potential (mV)	EE %	LE %
ZRL (1:1)	309 ± 10	0.15 ± 0.06	− 24.61 ± 1.71	–	–
ZRL (1:2)	354 ± 21	0.43 ± 0.06	− 30.42 ± 1.23	–	–
ZRL (1:0.5)	291 ± 6	0.29 ± 0.02	− 21.11 ± 1.01	–	–
CRZRL	276 ± 10	0.24 ± 0.07	− 29.13 ± 1.60	95.50 ± 2.65	41.61 ± 1.16

± values are considered in triplicate measurements

matrix as compared to others like chitosan (Dai et al. 2018). Furthermore, the method applied to encapsulate the compound should also be highly efficient as the case with antisolvent precipitation leading to a 95% EE and 42% LE which is the highest LE than any previous reports for zein nanoformulation in zein matrices (Wu et al. 2012), zein, and rhamnolipid complex (Dai et al. 2018) and also in chitosan (Keawchaoon and Yoksan 2011). The higher EE and LE could be due to strong electrostatic interaction, hydrogen bonding, and hydrophobic interaction between carvacrol, zein, and rhamnolipid which improved the embedding ability of the colloidal particles (Dai et al. 2018) which is also supported by our docking studies. The higher LE of loaded carvacrol as compared to other previous studies could also be due to the smaller size and higher solubility of carvacrol in absolute alcohol as compared to other botanicals or phytoconstituents (Dai et al. 2019).

Morphological study by FE-SEM

The morphology of the samples was analyzed by FE-SEM (Fig. 1). Both the CRZRL and ZRL showed the features of spherical shapes with smooth surfaces. The carvacrol-loaded CRZRL had a smaller size of 271 nm as compared to ZRL with a larger size of 306 nm which is as per our DLS data. Interestingly, the carvacrol encapsulation had a major influence in the size but there was no influence in the shape of the complex nanoparticles which could be due to stronger steric repulsion and hydrophobic interactions among the particles (Keawchaoon and Yoksan 2011; Wang and Zhang 2017). There was no visible aggregation in the carvacrol-loaded CRZRL as reported previously (Keawchaoon and Yoksan 2011; Zhang et al. 2014).

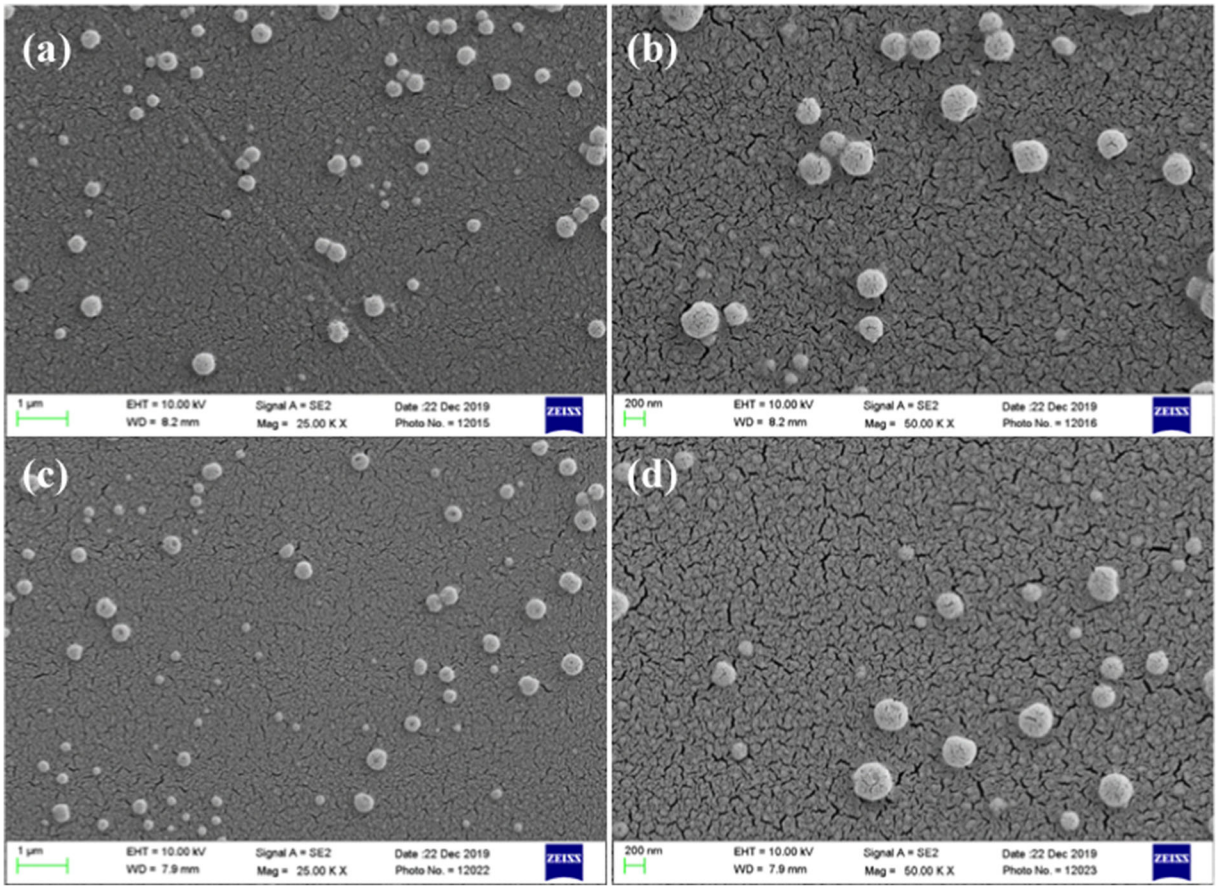

Fig. 1 FE-SEM micrographs of ZRL (**a**, **b**) and CRZRL (**c**, **d**)

Thermal study by DSC

The thermal stability of each component and complex nanoparticles was investigated by DSC (Fig. 2). The DSC thermograms of CR, CRZRL, ZRL, and RL showed broad endothermic peaks at 184, 68, 73, 132, and 225 °C. Compared to the RL, there is only one peak at 73 °C in ZRL indicating that the thermal stability of the zein and rhamnolipid has been improved (Wei et al. 2019). The presence of only a single endothermic peak at 68 °C in CRZRL indicates that carvacrol was well dispersed and encapsulated in zein/rhamnolipid complex nanoparticles (Wei et al. 2019).

Functional group study by FTIR

Investigation of the chemical structure and the interactions between zein, rhamnolipid, and carvacrol were studied by FTIR spectroscopy. The FTIR spectra of CR, CRZRL, ZRL, and RL were shown in Fig. 3. The native spectra of carvacrol and rhamnolipid showed characteristic peaks of O-H stretching bands at 3408 and 3361 cm^{-1} respectively which was shifted to 3388 cm^{-1} in the case of ZRL and CRZRL. The two major characteristic peaks of zein manifested in terms of amide I band (1750–1600 cm^{-1}) and amide II bands (1550–1510 cm^{-1}) correspond to C=O and C-N stretching, respectively. These major characteristic peaks of zein were observed at 1659 and 1545 cm^{-1} in

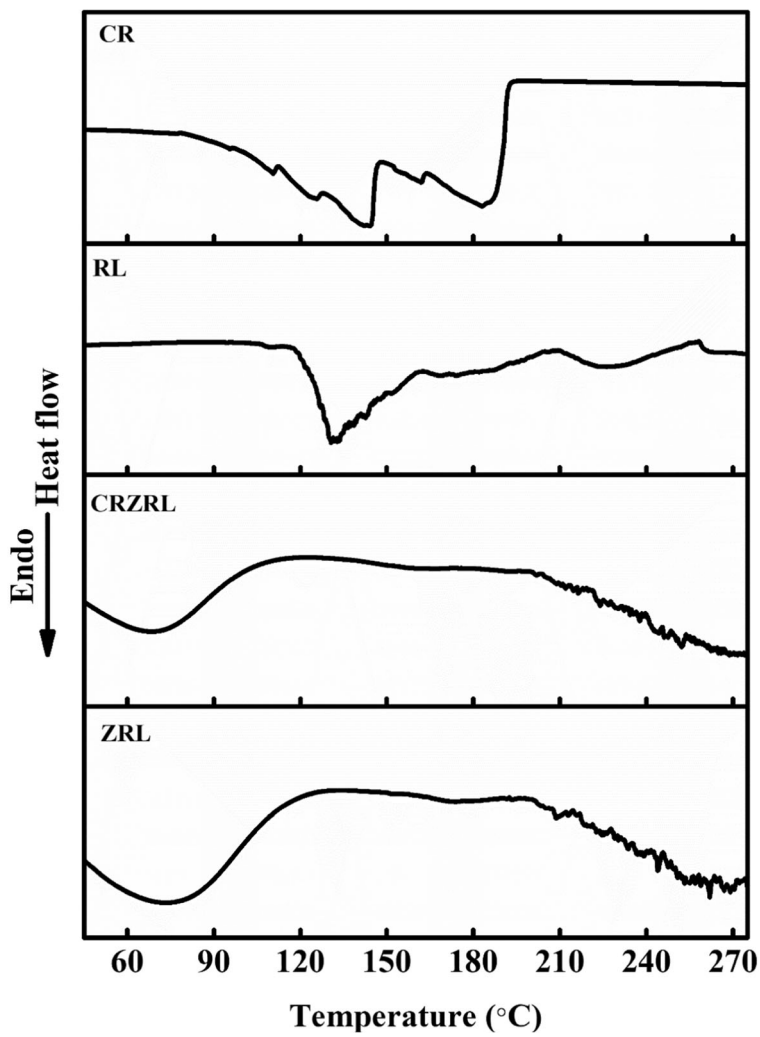

Fig. 2 Thermal studies of ZRL, CRZRL, RL, and CR by DSC

ZRL and 1651 and 1543 cm^{-1} in CRZRL which indicates electrostatic interaction between zein, rhamnolipid, and carvacrol (Keawchaoon and Yoksan 2011; Dai et al. 2018; Wei et al. 2019). The significant peak of C-H stretching at 2962 and 2872 cm^{-1} that were present in CR is shifted and observed at 2968, 2921, and 2881 cm^{-1} for CRZRL. The C-H stretching was also observed at 2928 and 2862 cm^{-1} in ZRL and 2928 and 2856 cm^{-1} in RL (Keawchaoon and Yoksan 2011; Dai et al. 2018; Wei et al. 2019). Furthermore, the characteristic peaks of carvacrol (CR) at 1455 and 1259 cm^{-1} are due to C-H deformation and the peaks of the aromatic ring at 867 and 816 cm^{-1} (Keawchaoon and Yoksan 2011). In the spectra of CRZRL, there is a slight shifting of C-H deformation at 1451 and 1252 cm^{-1} and also an aromatic ring at 872 cm^{-1}. The characteristic peak for rhamnolipid was C–O stretching vibration due to ether bonds (Wei et al. 2019) which is observed at 1066 and 1060 cm^{-1} in the spectra of RL and ZRL respectively (Fig. 3). The C-H stretching in CRZRL (2968, 2921, and 2881 cm^{-1}) suggests the successful encapsulation of carvacrol (Keawchaoon and Yoksan 2011). These results observed in the spectra of CR, CRZRL, ZRL, and RL revealed that hydrogen bonding, hydrophobic effects, and electrostatic interactions of zein and rhamnolipid with carvacrol contributed to the formation of carvacrol-loaded CRZRL (Dai et al. 2018; Wei et al. 2019) which was also supported by binding affinity results depicted by molecular docking studies.

H-bond study by H^1NMR

The presence of carvacrol, rhamnolipid, zein, and their interactions were confirmed by H^1NMR spectroscopy (Fig. 4 and Table ST1). In the spectrum of carvacrol (CR) characteristic peak signal at δ 7.0 ppm (Ar-H), 6.7 and 6.6 ppm (Ar-OH), 4.9 ppm (H attached to alkene C=CH), 2.9–2.4 ppm (Aromatic methyl, Ar-CH_3), and 1.8–1.2 ppm (Alkyl tertiary, H-CR_3) (Locci et al. 2004). The spectrum of rhamnolipid (RL) showed signal peak δ 5.3 ppm (-CH-OOC- on rhamnose moiety), 4.8–4.1 ppm (-CH_2-O- on rhamnose moiety), 3.6 ppm (-

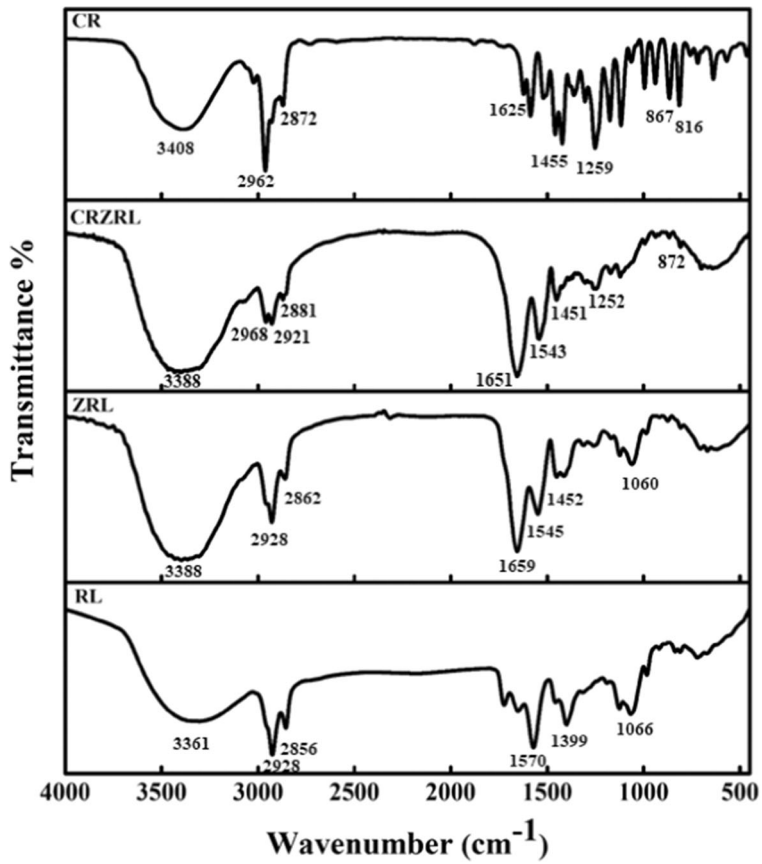

Fig. 3 FTIR spectra of pure carvacrol (CR), carvacrol-loaded zein NPs (CRZRL), unloaded zein NPs (ZRL), and rhamnolipid (RL)

CH2-CHO-Rha-CH2COO on β-hydroxyfatty acids), 3.3 ppm (-CH-OH on rhamnose moiety), 2.8–2.3 ppm (-CHO-CH2COO on β-hydroxyfatty acids), 1.6–1.4 ppm (-CH2-CHO-CH2COO on β-hydroxyfatty acids), 1.1 ppm (-CH3 on rhamnose moiety), and 0.8 ppm (-CH3 on β-hydroxyfatty acids) (Lotfabad et al. 2010; Moussa et al. 2014). The signal peaks of zein powder have already been mentioned in our previous study (Devi et al. 2019). The shifting of the signal peak at 5.4 (-CH-OOC- on rhamnose moiety), 4.9–4.2 ppm (-CH2-O- on rhamnose moiety), 3.7 ppm (-CH2-CHO-Rha-CH2COO on β-hydroxyfatty acids), 3.4–3.1 ppm (-CH-OH on rhamnose moiety), 2.4–2.0 ppm (-CHO-CH2COO on β-hydroxyfatty acids of rhamnolipid and –CH of –NH of zein), 1.7–1.3 ppm (-CH2-CHO-CH2COO on β-hydroxyfatty acids of rhamnolipid and –CH2- of zein), 1.2 ppm (-CH3 on rhamnose moiety), and 0.9 ppm (-CH3 on β-hydroxyfatty acids) were observed in the spectrum of ZRL. And also in the spectrum of CRZRL, a signal peak was observed at δ 6.9 ppm (Ar-H of carvacrol), 6.6–6.5 ppm (Ar-OH of carvacrol), 5.2 ppm (-CH-OOC- on rhamnose moiety of rhamnolipid), 2.9 ppm (Aromatic methyl, Ar-CH_3 of carvacrol and -CHO-CH2COO on β-hydroxyfatty acids of rhamnolipid), − 2.4 ppm (Aromatic methyl, Ar-CH_3 and -CHO-CH2COO on β-hydroxyfatty acids of rhamnolipid), and 1.9 ppm (-CH2-CHO-CH2COO on β-hydroxyfatty acids of rhamnolipid, Alkyl tertiary, H-CR_3 of carvacrol and –CH2- of zein), 1.2 ppm (Alkyl tertiary, H-CR_3 of carvacrol, -CH2-CHO-CH2COO on β-hydroxyfatty acids of rhamnolipid and –CH2- of zein), 1.1 ppm (-CH3 on rhamnose moiety and Alkyl tertiary, H-CR_3 of carvacrol), and 0.9 ppm (-CH3 on β-hydroxyfatty acids). The slight shift of δ values of ± 0.1 ppm proved that among the encapsulated carvacrol, zein, and rhamnolipid, there must be hydrophobic interaction and hydrogen interaction and hydrogen bonding as given in Fig. 4 and Table ST1 (Supporting Information). Thus, from the results obtained including FTIR, DSC, and H^1NMR, it can be considered that carvacrol is encapsulated successfully in the zein/rhamnolipid (ZRL) complex nanoparticles.

Docking studies

The molecular docking studies with carvacrol and rhamnolipid show the different binding and pocket sites for the zein protein in Table 2. We also performed multiple ligand simultaneous docking which helps in a deeper understanding of the combined effect of interaction between carvacrol and rhamnolipid with zein protein. Each docking shows 9 (nine) conformation of binding pockets for targeting sites shown in Fig. 5 and Fig. ES4 (Supporting Information). Docking study results for the binding of these compounds are shown in Table 2, Fig. 5, and in Fig. ES4 (Supporting Information). Each conformation has a different binding affinity, w.r.t, the root mean square deviation (rmsd) value of the lower base and upper base.

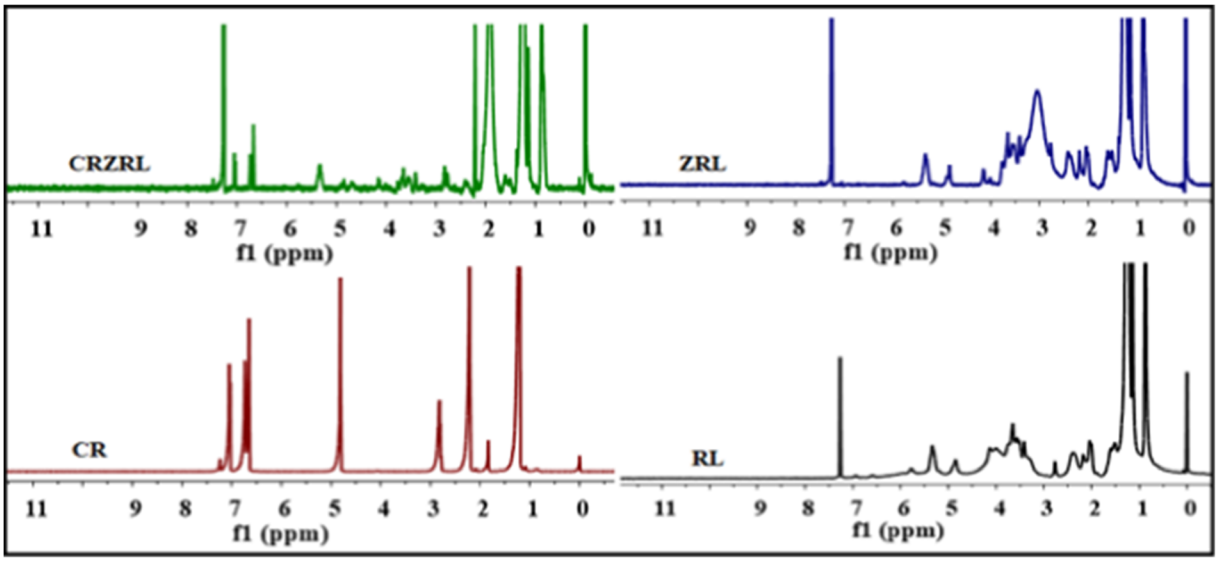

Fig. 4 Chemical shift analysis of carvacrol-loaded (CRZRL), carvacrol (CR), ZRL, and rhamnolipid (RL) by ^{1}H NMR spectra

Table 2 Highest docking scores of different compounds with active site residues of zein

List of compounds	Highest binding E\energy (ΔG) (Kcal/mol)	Active site residues	Bond strength (Å)
Carvacrol	− 5.8	GLN-84, GLN-277	3.3, 2.5
Rhamnolipid	− 7.4	ARG-218, ASN-251	2.8, 3.0
Rhamnolipid + carvacrol	− 5.8	GLN-84, ARG-218, ASN-251, VAL-232	5.2,5.4, 5.8, 5.2

Zein has different active binding or targeting sites for both compounds but while performing multiple ligand simultaneous docking, we found some common active sites which show the interaction behavior for both compounds together at the same time. The detailed description of active binding or targeting sites for each compound are shown in Table 2. Furthermore, the analysis of the molecular docking reveals that the rhamnolipid has stronger interactions and binding affinity with the zein protein in comparison with carvacrol. The highest binding affinity of carvacrol was around − 5.8 Kcal/mol while the rhamnolipid recorded the highest binding affinity of − 7.4 Kcal/mol. When we performed multiple ligand simultaneous docking with carvacrol and rhamnolipid, they showed the highest binding affinity of − 5.8 Kcal/mol. This binding affinity was equal with the carvacrol binding affinity, but due to the presence of rhamnolipid, we found the more selective binding site. These binding sites show Π-Π interaction, which depicts the stronger interactions and binding affinity of carvacrol and rhamnolipid with the zein protein (Fig. 5 and Fig. ES4 (Supporting Information)).

Antimicrobial activity of carvacrol-loaded zein/rhamnolipid complex nanoparticles

In vitro study of antibacterial and antifungal activity of CRZRL against *P. syringae* and *F. oxysporum* is given in Fig. 6 a and b and in supporting information Figs. ES1 and ES2. MICs of CRZRL against *P. syringae* and *F. oxysporum* are 135 μg/mL and 270 μg/mL respectively (Fig. 6a, b). The antibacterial and the antifungal

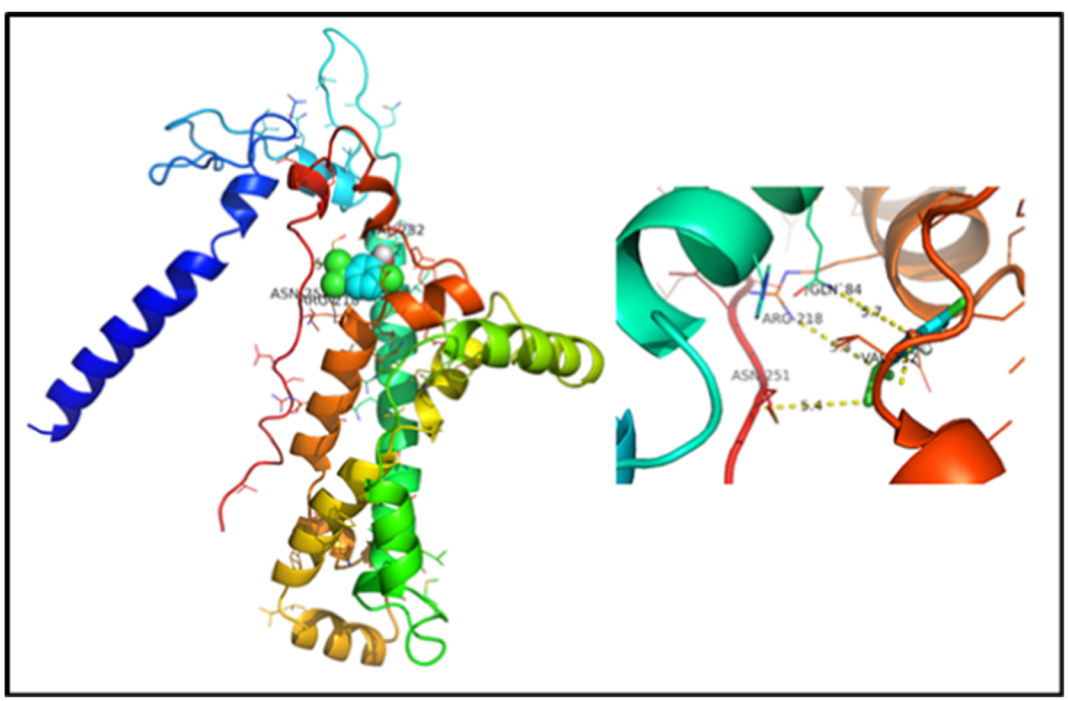

Fig. 5 The interaction between carvacrol and rhamnolipid compounds with the active site of the zein protein at GLN-84, ARG-218, ASN-251, VAL-232

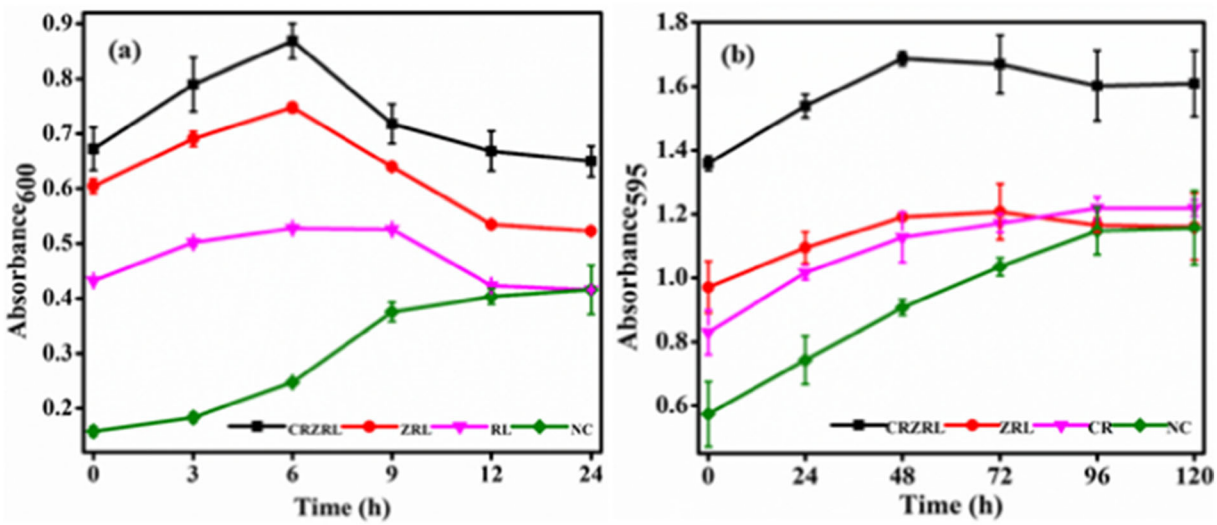

Fig. 6 **a**) Antibacterial and **b** Antifungal activity of CRZRL, ZL, CR, and NC against *P. syringae* and *F. oxysporum*. Negative control (NC) represents the absorbance of the suspension of *P. syringae* without adding nanoparticles. Error bars indicate the standard deviations from three replicates

activities of CRZRL are comparatively higher than the free carvacrol and ZRL. Since rhamnolipid is a biosurfactant and its activity against few bacteria including some foodborne pathogens, e.g., *L. monocytogenes*, *B. cereus*, *S. aureus*, *E. coli* have been reported previously (de Freitas Ferreira et al. 2019) suggesting its pH-dependent antibacterial activity against gram-negative bacteria. Besides, this antifungal activity of rhamnolipid against *F. verticilliodes* (Borah et al. 2016) was also reported. Previously, many reports (namely da Rosa et al. 2015; Rao et al. 2020) had reported antimicrobial activity of carvacrol and carvacrol-loaded nanoparticles against *B. cereus*, *L. monocytogenes*, *S. aureus, E. coli*, *Salmonella*, and *S. enterica* and also against fungi (*B. cinerea*, *Aspergillus* spp., *Cladosporium* spp., etc.) (Martínez-Romero et al. 2007; Abbaszadeh et al. 2014). The antimicrobial activity of carvacrol might be due to the interaction of lipophilic carvacrol with microbial phospholipid cell membrane components leading to drastic changes in the cell membrane. The distortion of the structure would induce expansion, destabilization of the membrane, and increase membrane fluidity, which would eventually increase passive permeability (Cristani et al. 2007; Keawchaoon and Yoksan 2011; Rao et al. 2020). The enhanced antibacterial and antifungal activity of encapsulated carvacrol CRZRL may be due to the synergistic effect of rhamnolipid and zein. The activity of CRZRL against *P. syringae* is not much high as compared to ZRL which could be due to the lower susceptibility of hydrophobic compounds against gram-negative microorganisms because of their restricted diffusion across lipopolysaccharides present on the outer membrane (Burt 2004). The primary action of the carvacrol at the membrane and inside the cytoplasm was improved as compared to the previous studies (Wang et al. 2011) which may be likely because rhamnolipid enhanced the access of carvacrol to these regions by increasing carvacrol aqueous solubility (Rao et al. 2020). Although the antimicrobial effect of carvacrol is reported previously, its activity against phytopathogens like *P. syringae* and *F. oxysporum* for preventing plant diseases using zein-based nanoparticles stabilized by rhamnolipid is yet to be reported. The selected organisms have also been studied in our previous work (Devi et al. 2019) showing the antimicrobial potential of rotenone-loaded zein nanoparticles which are stabilized by sodium caseinate.

Thus, phytoconstituents like carvacrol can be used in lower concentrations in the form of nanoformulation with improved antimicrobial activity against various pathogenic microorganisms giving an exciting area for future research.

Conclusions

The rhamnolipid stabilized zein-based complex nanoparticles prepared with carvacrol encapsulation was

confirmed by FTIR, H^1NMR, DSC, and molecular docking analysis. The active sites (amino acids) of zein determined from docking studies correlate with the results from FTIR where characteristic peaks of amide I band (1750–1600 cm^{-1}) and amide II bands (1550–1510 cm^{-1}) corresponding to C=O and C-N stretching respectively was shifted to 1651 and 1543 cm^{-1} in CRZRL indicating the involvement of electrostatic interaction between zein, rhamnolipid, and carvacrol and its successful encapsulation. Besides carvacrol encapsulation, its homogenous dispersion in CRZRL was confirmed by the absence of endothermic peak at 184 °C as discussed previously in our DSC results. Further, the chemical shift obtained from H^1NMR spectra indicated the interactions among carvacrol, rhamnolipid, and zein. This led to the enhancement in EE% and LE% and increased aqueous solubility of carvacrol. The observed MIC value of 135 μg/mL and 270 μg/mL against *P. syringae* and *F. oxysporum* respectively, responsible for bacterial canker and fusarium wilt in plants and crops, could be controlled by the prepared carvacrol-loaded nano-formulation and thus can be used to manage other plant diseases also. Further such kind of prepared nano formulation could also find application in food packaging material to control various foodborne pathogens.

Acknowledgments Ngangom Bidyarani would like to thank Central University of Gujarat for allowing accessibility to Central Instrumentation Facility (CIF-CUG) to complete this research work and Dr. Prajesh Prajapati, Assistant Professor, Gujarat Forensic Sciences University for HPLC studies.

Compliance with ethical standards

Conflict of interest The authors declare that they have no conflict of interest.

References

Abbaszadeh S, Sharifzadeh A, Shokri H, Khosravi AR, Abbaszadeh A (2014) Antifungal efficacy of thymol, carvacrol, eugenol and menthol as alternative agents to control the growth of food-relevant fungi. J Mycol Med 24:e51–e56. https://doi.org/10.1016/j.mycmed.2014.01.063

Bai L, McClements DJ (2016) Formation and stabilization of nanoemulsions using biosurfactants: rhamnolipids. J Colloid Interface Sci 479:71–79. https://doi.org/10.1016/j.jcis.2016.06.047

Borah SN, Goswami D, Sarma HK et al (2016) Rhamnolipid biosurfactant against Fusarium verticillioides to control stalk and ear rot disease of maize. Front Microbiol 7:1505

Broekaert WF, Terras FRG, Cammue BPA, Vanderleyden J (1990) An automated quantitative assay for fungal growth inhibition. FEMS Microbiol Lett 69:55–59. https://doi.org/10.1111/j.1574-6968.1990.tb04174.x

Burt S (2004) Essential oils: their antibacterial properties and potential applications in foods—a review. Int J Food Microbiol 94:223–253. https://doi.org/10.1016/j.ijfoodmicro.2004.03.022

Camo J, Lorés A, Djenane D, Beltrán JA, Roncalés P (2011) Display life of beef packaged with an antioxidant active film as a function of the concentration of oregano extract. Meat Sci 88:174–178. https://doi.org/10.1016/j.meatsci.2010.12.019

Casas-Flores S, Domínguez-Espíndola RB, Camposeco-solis R, Patrón-Soberano OA, Rodríguez-González V (2019) Unraveling the photoactive annihilation mechanism of nanostructures as effective green tools for inhibiting the proliferation of the phytopathogenic bacterium Pseudomonas syringae. Nanoscale Adv 1:2258–2267. https://doi.org/10.1039/C8NA00307F

Cristani M, D'Arrigo M, Mandalari G et al (2007) Interaction of four monoterpenes contained in essential oils with model membranes: implications for their antibacterial activity. J Agric Food Chem 55:6300–6308. https://doi.org/10.1021/jf070094x

da Rosa CG, de Oliveira Brisola Maciel MV, de Carvalho SM, de Melo APZ, Jummes B, da Silva T, Martelli SM, Villetti MA, Bertoldi FC, Barreto PLM (2015) Characterization and evaluation of physicochemical and antimicrobial properties of zein nanoparticles loaded with phenolics monoterpenes. Colloids Surf A Physicochem Eng Asp 481:337–344. https://doi.org/10.1016/j.colsurfa.2015.05.019

Dai L, Li R, Wei Y, Sun C, Mao L, Gao Y (2018) Fabrication of zein and rhamnolipid complex nanoparticles to enhance the stability and in vitro release of curcumin. Food Hydrocoll 77:617–628. https://doi.org/10.1016/j.foodhyd.2017.11.003

Dai L, Zhou H, Wei Y, Gao Y, McClements DJ (2019) Curcumin encapsulation in zein-rhamnolipid composite nanoparticles using a pH-driven method. Food Hydrocoll 93:342–350. https://doi.org/10.1016/j.foodhyd.2019.02.041

de Freitas Ferreira J, Vieira EA, Nitschke M (2019) The antibacterial activity of rhamnolipid biosurfactant is pH dependent. Food Res Int 116:737–744. https://doi.org/10.1016/j.foodres.2018.09.005

Del Nobile MA, Conte A, Incoronato AL, Panza O (2008) Antimicrobial efficacy and release kinetics of thymol from zein films. J Food Eng 89:57–63. https://doi.org/10.1016/j.jfoodeng.2008.04.004

Devi N, Bidyarani N, Kumar U (2019) Synthesis of rotenone loaded zein nano-formulation for plant protection against pathogenic microbes. RSC Adv 9:40819–40826. https://doi.org/10.1039/C9RA08739G

Dwivedi S, Saquib Q, Al-Khedhairy AA et al (2015) Rhamnolipids functionalized AgNPs-induced oxidative stress and modulation of toxicity pathway genes in cultured MCF-7 cells. Colloids Surf B: Biointerfaces 132:290–298. https://doi.org/10.1016/j.colsurfb.2015.05.034

Fones H, Preston GM (2013) The impact of transition metals on bacterial plant disease. FEMS Microbiol Rev 37:495–519. https://doi.org/10.1111/1574-6976.12004

Fuhrmann J, Rurainski A, Lenhof H-P, Neumann D (2010) A new Lamarckian genetic algorithm for flexible ligand-receptor docking. J Comput Chem 31:1911–1918. https://doi.org/10.1002/jcc.21478

Guarda A, Rubilar JF, Miltz J, Galotto MJ (2011) The antimicrobial activity of microencapsulated thymol and carvacrol. Int J Food Microbiol 146:144–150. https://doi.org/10.1016/j.ijfoodmicro.2011.02.011

Hirano SS, Upper CD (2000) Bacteria in the leaf ecosystem with emphasis onPseudomonas syringae—a pathogen, ice nucleus, and epiphyte. Microbiol Mol Biol Rev 64:624 LP–624653. https://doi.org/10.1128/MMBR.64.3.624-653.2000

Keawchaoon L, Yoksan R (2011) Preparation, characterization and in vitro release study of carvacrol-loaded chitosan nanoparticles. Colloids Surf B: Biointerfaces 84:163–171. https://doi.org/10.1016/j.colsurfb.2010.12.031

Li F, Chen Y, Liu S, Qi J, Wang W, Wang C, Zhong R, Chen Z, Li X, Guan Y, Kong W, Zhang Y (2017) Size-controlled fabrication of zein nano/microparticles by modified anti-solvent precipitation with/without sodium caseinate. Int J Nanomedicine 12:8197–8209. https://doi.org/10.2147/IJN.S143733

Locci E, Lai S, Piras A, Marongiu B, Lai A (2004) 13C-CPMAS and 1H-NMR study of the inclusion complexes of β-cyclodextrin with carvacrol, thymol, and eugenol prepared in supercritical carbon dioxide. Chem Biodivers 1:1354–1366. https://doi.org/10.1002/cbdv.200490098

Lotfabad TB, Abassi H, Ahmadkhaniha R, Roostaazad R, Masoomi F, Zahiri HS, Ahmadian G, Vali H, Noghabi KA (2010) Structural characterization of a rhamnolipid-type biosurfactant produced by Pseudomonas aeruginosa MR01: enhancement of di-rhamnolipid proportion using gamma irradiation. Colloids Surf B: Biointerfaces 81:397–405. https://doi.org/10.1016/j.colsurfb.2010.06.026

Martínez-Romero D, Guillén F, Valverde JM et al (2007) Influence of carvacrol on survival of Botrytis cinerea inoculated in table grapes. Int J Food Microbiol 115:144–148. https://doi.org/10.1016/j.ijfoodmicro.2006.10.015

Mastromatteo M, Danza A, Conte A, Muratore G, del Nobile MA (2010) Shelf life of ready to use peeled shrimps as affected by thymol essential oil and modified atmosphere packaging. Int J Food Microbiol 144:250–256. https://doi.org/10.1016/j.ijfoodmicro.2010.10.002

Moussa TAA, Mohamed MS, Samak N (2014) Production and characterization of di-rhamnolipid produced by Pseudomonas aeruginosa TMN. Braz J Chem Eng 31:867–880

de Oliveira JL, Campos EVR, Pereira AES et al (2018) Zein nanoparticles as eco-friendly carrier systems for botanical repellents aiming sustainable agriculture. J Agric Food Chem 66:1330–1340. https://doi.org/10.1021/acs.jafc.7b05552

Paliwal R, Palakurthi S (2014) Zein in controlled drug delivery and tissue engineering. J Control Release 189:108–122. https://doi.org/10.1016/j.jconrel.2014.06.036

Ramos M, Jiménez A, Peltzer M, Garrigós MC (2012) Characterization and antimicrobial activity studies of polypropylene films with carvacrol and thymol for active packaging. J Food Eng 109:513–519. https://doi.org/10.1016/j.jfoodeng.2011.10.031

Rao S, Xu G, Lu X, Zhang R, Gao L, Wang Q, Yang Z, Jiao X (2020) Characterization of ovalbumin-carvacrol inclusion complexes as delivery systems with antibacterial application. Food Hydrocoll 105:105753. https://doi.org/10.1016/j.foodhyd.2020.105753

Rhein LD, Schlossman M, O'Lenick A, Somasundaran P (2006) Surfactants in personal care products and decorative cosmetics. Crc press, Boca Raton

Riella KR, Marinho RR, Santos JS, Pereira-Filho RN, Cardoso JC, Albuquerque-Junior RLC, Thomazzi SM (2012) Anti-inflammatory and cicatrizing activities of thymol, a monoterpene of the essential oil from Lippia gracilis, in rodents. J Ethnopharmacol 143:656–663. https://doi.org/10.1016/j.jep.2012.07.028

Srivastav AK, Gupta SK, Kumar U (2020) A molecular simulation approach towards the development of universal nanocarriers by studying the pH-and electrostatic-driven changes in the dynamic structure of albumin. RSC Adv 10:13451–13459

Trott O, Olson AJ (2010) AutoDock Vina: improving the speed and accuracy of docking with a new scoring function, efficient optimization, and multithreading. J Comput Chem 31:455–461. https://doi.org/10.1002/jcc.21334

van der Wolf J, De Boer SH (2015) Phytopathogenic bacteria BT - principles of plant-microbe interactions: microbes for sustainable agriculture. In: Lugtenberg B (ed). Springer International Publishing, Cham, pp 65–77

Wang L, Zhang Y (2017) Eugenol nanoemulsion stabilized with zein and sodium caseinate by self-assembly. J Agric Food Chem 65:2990–2998. https://doi.org/10.1021/acs.jafc.7b00194

Wang T, Li B, Si H, Lin L, Chen L (2011) Release characteristics and antibacterial activity of solid state eugenol/β-cyclodextrin inclusion complex. J Incl Phenom Macrocycl Chem 71:207–213. https://doi.org/10.1007/s10847-011-9928-3

Weerakkody NS, Caffin N, Turner MS, Dykes GA (2010) In vitro antimicrobial activity of less-utilized spice and herb extracts against selected food-borne bacteria. Food Control 21:1408–1414. https://doi.org/10.1016/j.foodcont.2010.04.014

Wei Y, Yu Z, Lin K, Sun C, Dai L, Yang S, Mao L, Yuan F, Gao Y (2019) Fabrication and characterization of resveratrol loaded zein-propylene glycol alginate-rhamnolipid composite nanoparticles: physicochemical stability, formation mechanism and in vitro digestion. Food Hydrocoll 95:336–348. https://doi.org/10.1016/j.foodhyd.2019.04.048

Wu Y, Luo Y, Wang Q (2012) Antioxidant and antimicrobial properties of essential oils encapsulated in zein nanoparticles prepared by liquid–liquid dispersion method. LWT Food Sci Technol 48:283–290. https://doi.org/10.1016/j.lwt.2012.03.027

Zhang Y, Niu Y, Luo Y, Ge M, Yang T, Yu L(L), Wang Q (2014) Fabrication, characterization and antimicrobial activities of thymol-loaded zein nanoparticles stabilized by sodium caseinate–chitosan hydrochloride double layers. Food Chem 142:269–275. https://doi.org/10.1016/j.foodchem.2013.07.058